Raman scattering in multiferroic $SmFe_3(BO_3)_4$

Cite as: Low Temp. Phys. **42**, 475 (2016); https://doi.org/10.1063/1.4954783
Submitted: 20 January 2016 . Accepted: 13 June 2016 . Published Online: 07 July 2016

A. V. Peschanskii, V. I. Fomin, and I. A. Gudim

LOW-TEMPERATURE OPTICAL SPECTROSCOPY

Raman scattering in multiferroic $SmFe_3(BO_3)_4$

A. V. Peschanskii[a] and V. I. Fomin

B. Verkin Institute for Low Temperature Physics and Engineering of the National Academy of Sciences of Ukraine, 47 Nauki Ave., Kharkov 61103, Ukraine

I. A. Gudim

L. V. Kirenskii Institute of Physics, Siberian Branch of the Russian Academy of Sciences, Krasnoyarsk 660036, Russia

(Submitted January 20, 2016)
Fiz. Nizk. Temp. **42**, 607–618 (June 2016)

Raman spectrum of single-crystal $SmFe_3(BO_3)_4$ was studied in the frequency range from 3 to 1500 cm^{-1} at temperatures 10–300 K. All the A_1 and E phonon modes predicted by the group theory for a given symmetry of the crystal were observed. The magnitudes of splitting between the LO and TO components of polar E phonons were determined. It was found that under the transition to a magnetically ordered phase, the behavior of the intensity of the line corresponding to the A_1 vibrational mode is anomalous. It was shown that at low temperatures the spectrum of two-magnon excitations has a complex shape and is observed with both nondiagonal and diagonal components of the scattering tensor. This complex shape reflects the features in the density of states of the magnetic branches. An estimate of the magnon energy E_m at the Brillouin zone boundary gave $\sim$47 cm^{-1}. The structure of the ground multiplet $^6H_{5/2}$ of a Sm^{+3} ion in paramagnetic and antiferromagnetic states as well as the effect of the magnetic phase transition on it were studied. Electron-phonon interaction for the electronic excitation at 225 cm^{-1} was revealed. *Published by AIP Publishing.* [http://dx.doi.org/10.1063/1.4954783]

Introduction

In recent years, the physical properties of multiferroics from the $ReFe_3(BO_3)_4$ (Re = La–Lu) ferroborate family have been actively investigated, both theoretically and experimentally.[1–4] This is related to the discovery of large magnetoelectric effect in these compounds, which allows to control their electrical properties with an external magnetic field. Among the studied rare-earth ferroborates, $SmFe_3(BO_3)_4$ is special due to spontaneous electric polarization arising in the magnetically ordered phase, which can reach a magnitude of about 500 $\mu C/m^2$ in a magnetic field.[5,6] The large spontaneous polarization below T_N is observed in the basal plane.

$SmFe_3(BO_3)_4$ crystallizes in the trigonal system with space group $R32$ (D_3^7). This structure is maintained down to 2 K.[7] The antiferromagnetic ordering of Fe^{3+} ions occurs at $T_N = 33$ K.[7] The magnetic moments of iron ions are oriented in the basal *ab*-plane perpendicular to the *c*-axis of the crystal. Below $T_N = 33$ K, both samarium and iron ion sublattices are ferromagnetically ordered within the basal *ab*-plane, while in the adjacent layers in the axial direction, the magnetic moments are antiferromagnetically ordered. Easy-plane behavior of the antiferromagnetic structure at $T < T_N$ has been revealed in neutron scattering experiments on $SmFe_3(BO_3)_4$ powder.[7] It is established that the unit cell is doubled along the *c*-axis in the magnetically ordered state. The relative orientation of the magnetic moments of iron and samarium ions has not been clearly established. According to the neutron diffraction data, the misalignment angle between the iron and samarium sublattices in the basal *ab*-plane is 70°,[7] while a collinear magnetic structure is considered to be more preferable.[8] In the latter case, the emergence of domains with different orientations of the magnetic moments of iron and samarium ions along one of the three possible directions of the *a*-axis is expected at $T < T_N$.

Quantum theory of magnetoelectricity in rare ferroborates has been developed in Ref. 4. It has been shown that electric polarization in the materials is realized through two single-ion mechanisms: the effective magnetic and crystal fields induce an electric dipole moment directly in the 4*f*-shell of rare-earth ions (electric contribution). Besides that, the displacement of oppositely charged ionic sublattices also contributes to the appearance of the phenomenon (ion contribution). The magnetoelectric properties have been described in detail for neodymium, samarium and europium ferroborates. The field and temperature dependences of polarization have been obtained.

In order to describe the magnetoelectric properties of rare-earth materials, it is necessary to have the information on the energy spectrum and wave functions of rare-earth ions in the crystal. The energy levels of Sm^{3+} ions in the paramagnetic phase of crystal $SmFe_3(BO_3)_4$ and the effect of the magnetic ordering on the energy levels have been studied in Refs. 8 and 9 using absorption spectra. The spectroscopic studies of rare-earth ferroborates with Re = Nd, Sm, and Gd in the submillimeter region have revealed the presence of resonant magnetic excitations in the exchange-interacting antiferromagnetic (Fe) and paramagnetic (Re) subsystems and identified a number of specific features of their dynamics.[10] It has been found that a strong interaction between the spin

fluctuations of Fe and Sm sublattices is present, forming a coupled excitation spectrum, which depends on the type of Re ion and the anisotropy of exchange splitting of its ground state (doublet). In $SmFe_3(BO_3)_4$, where Sm^{3+} ions interact very weakly with an external magnetic field, the excitation of exchange (Sm) modes is associated with the Fe subsystem.[10]

Raman spectra of several $ReFe_3(BO_3)_4$ (Re = Gd, Nd, Tb, Er, and Y) crystals have been studied in a wide temperature range, covering various structural and magnetic phases.[11] For $TbFe_3(BO_3)_4$, external vibrational modes of the crystal lattice (below $500\,cm^{-1}$) and the spectrum of two-magnon excitations have been studied, and the effect of an external magnetic field on some vibrational excitations in the magnetically ordered phase has been revealed.[12] On the other hand, there is no Raman spectroscopy data on crystalline $SmFe_3(BO_3)_4$. The vibrational spectrum of this compound has only been studied by IR spectroscopy at room temperature.[13]

The present paper reports the results of a Raman spectral study of oriented single-crystal $SmFe_3(BO_3)_4$ in the paramagnetic and antiferromagnetic states. This work focuses on the structure of the ground multiplet $^6H_{5/2}$ of Sm^{3+} ion, the effect of magnetic ordering on it, the formation of two-magnon excitation spectrum, as well as finding the energy and symmetry of the vibrational excitations and a possible impact on them of the magnetic phase transition. This can clarify the nature of interaction between the subsystems, which defines unique magnetelectrical properties of these compounds.

Samples, measurement techniques and group-theory analysis of the vibrational excitations

Studies were performed on a $SmFe_3(BO_3)_4$ crystal of good optical quality grown from a molten solution based on bismuth trimolybdate as described in Ref. 14. The sample was cut in a cuboidal shape of $3.2 \times 4.7 \times 4.2$ mm with the faces thoroughly polished. The edges were parallel to the axes $Z \,||\, C_3$, $X \,||\, C_2$ and $Y \perp Z,X$. Orientation was carried out using the crystal habit and verified using the x-ray technique. Sample quality check was performed using a polarizing microscope. The orientation of the C_3-axis was within 1°.

Raman study was conducted in the 90° configuration. A 38 mW sold-state laser with $\lambda = 532$ nm was used for excitation. The scattered light was analyzed by a double monochromator Ramanor U-1000 and detected with a cooled photomultiplier RCA 31034 and photon-counting scheme. An optical cryostat, which held the sample immersed in helium vapor, allowed us to conduct research in a wide temperature range.

Raman spectra are presented in the standard notation $k(ij)q$, where k and q are the propagation directions of the incident and scattered light with the electric vector **e** along i and j, respectively. ZZ, XY, etc., notation correspond to specific components of the scattering tensor.

The crystal structure of $SmFe_3(BO_3)_4$ is R32 (D_3^7). The primitive cell contains one formula unit. Group-theory analysis of the vibrational excitations in rare-earth ferroborates has been described in Ref. 11. The lattice vibrations are described with $\Gamma_{vibr} = 7A_1 + 13A_2 + 20E$ symmetry types, including $\Gamma_{ac} = A_2 + E$ of the acoustic ones. $7A_1$ and doubly degenerate polar $19E$ modes are Raman-active; $12A_2 + 19E$ modes are IR-active. The non-zero components of the dispersion tensor for the above setting have the form: A_1—XX, YY, ZZ; E—XX, YY, YZ, ZY, XY, YX, XZ, ZX.[15]

The vibrational modes can be divided into the external $\Gamma_{ext} = 3A_1 + 8A_2 + 11E$ (with energies below $\sim 500\,cm^{-1}$) and internal vibrations of the BO_3 group $\Gamma_{int} = 4A_1 + 4A_2 + 8E$ (energy range of 500–1500 cm^{-1}). The energy ranges for a free ion BO_3 and the expected number of vibrational modes within these ranges are also known: $600\,cm^{-1}$ $\nu_4(E')$—$A_1 + 3E$; 700–800 cm^{-1} $\nu_2(A_2'')$—E; $950\,cm^{-1}$ $\nu_1(A_1')$—$2A_1 + E$; 1250–1400 cm^{-1} $\nu_3(E')$—$A_1 + 3E$).[11]

Experimental results and discussion

Figures 1 and 2 show the polarized Raman spectra at 10 K and similar spectra at room temperature in the range of internal and external vibrations of BO_3 groups, respectively. Spectra with ZZ-component of the scattering tensor allow to uniquely identify A_1 modes, while those with off-diagonal components help to separate E modes. Spectra with XX- and YY-components contain both A_1 and E modes.

As shown in Fig. 1(a), in the low-frequency region of the spectrum, a band with a complex structure is observed, which corresponds to two-magnon scattering, characteristic for the crystals of this family.[11,12] Furthermore, the dashed arrows in the figure indicate the lines corresponding to the electron transitions between the levels of the ground multiplet of Sm^{3+} ions. Before discussing in detail the two-magnon and electron scattering, let us consider the vibrational spectrum.

Vibrational modes

The spectral lines that remain up to room temperature are uniquely assigned to vibrational excitations. At low temperatures, these lines are narrow, allowing us to accurately determine the number of observed modes. As should be expected for a non-centrosymmetric crystals and has been shown in Refs. 11 and 12, for this class of compounds, the polar E modes split into the TO and LO components. For the spectra with $\theta = 90°$ (θ is the angle between the phonon propagation direction and the threefold axis) in this scattering geometry, the TO and LO components are observed at the same time (see the spectra in Figs. 1 and 2 in $Y(XY)X$, $Y(XZ)X$, and $Y(ZY)X$ scattering geometries). To separate the TO and LO components, different sample alignments is used, in which the propagation direction of a phonon is directed at an angle $\theta = 45°$ to the C_3 axis. Then, either only TO or LO components are observed (see the spectra in Figs. 1 and 2 in $Y(XX)Z$, $Y(XY)Z$, $Y(ZX)Z$, and $Y(ZY)Z$ geometries). At room temperature, in this scattering geometry, a complete separation of the components LO and TO (Fig. 2) is observed, while it is only preferable at low temperatures (Fig. 1). This is due to the fact that at low temperatures, linear-polarized light propagating along the Z-axis becomes elliptical and the mixing of the spectra with the components of the scattering tensor XX and XY, ZX, and ZY occurs.

It should also be noted that for $\theta = 45°$, the LO component is usually shifted to lower energies by half the value of the energy difference between the TO and LO components. This has been described in more detail in our paper[12] for

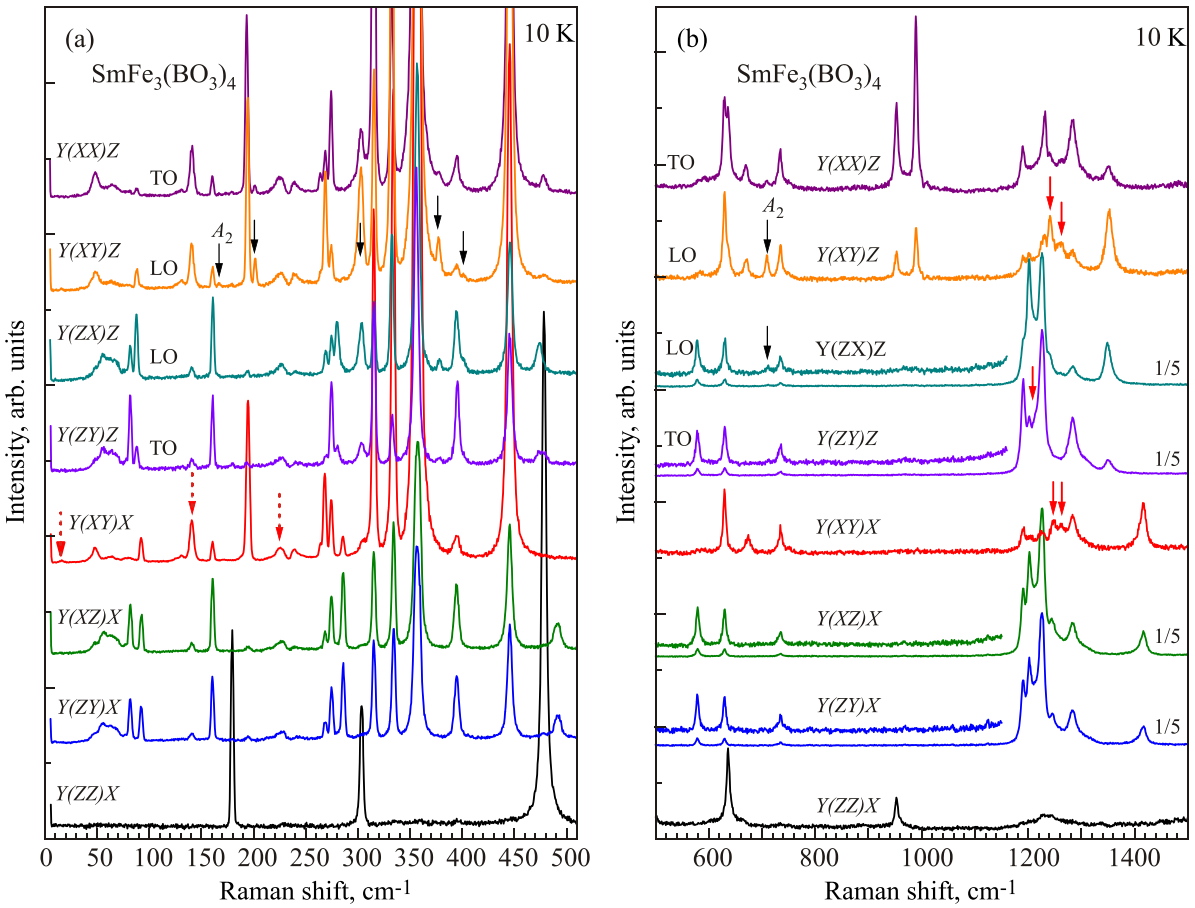

FIG. 1. Raman spectra of different polarizations observed in single-crystal $SmFe_3(BO_3)_4$ at 10 K in various geometries in the regions of external (a) and internal (b) BO_3 vibrational modes; $\lambda_{exc} = 532$ nm (38 mW); spectral resolution of 3.0 cm^{-1}.

$TbFe_3(BO_3)_4$ crystal. Separation into TO and LO components and shifting the LO component in the $\theta = 45°$ geometry is most clearly seen in Figs. 1 and 2 for the lowest and highest frequency E modes.

The energies of A_1 and E phonon modes for external and internal vibrations of BO_3 groups are shown in Tables 1 and 2, respectively. The error in determining the energy ranges is between ± 0.3 and ± 0.5 cm^{-1}, depending on the intensity of the lines. In addition to our data, Tables 1–3 show the results for isostructural crystals obtained by other authors.[11–13] As can be seen from Tables 1 and 2, all the $7A_1 + 19E$ vibrational modes predicted by group-theory analysis, including $3A_1 + 11E$ external and $4A_1 + 8E$ internal oscillations are observed in the spectrum. For a $SmFe_3(BO_3)_4$ crystal, which does not undergo a structural phase transition, the energy of most of the vibrational modes either does not change within the measurement accuracy or increases by several inverse centimeters with the temperature varying from 300 to 10 K, i.e., a normal temperature dependence is observed. The exception is E modes 93.2, 195.8, 954.0, and 1204.5 cm^{-1} (values for the LO component), the energy of which decreases with decreasing temperature (see Tables 1 and 2).

The energies of phonon modes and the splitting of several lines into the TO and LO components are similar to the respective data for $TbFe_3(BO_3)_4$ (Ref. 12) and $GdFe_3(BO_3)_4$ crystals.[11] In contrast, for $SmFe_3(BO_3)_4$ splitting into LO and TO components was observed for E modes: TO—264.3 cm^{-1} and LO—268.4 cm^{-1} (Table 1). A similar splitting has earlier been observed for a $NdFe_3(BO_3)_4$ crystal,[11] which also does not exhibit a structural phase transition. This difference between samarium ferroborate and the above crystals is likely related to the fact that at room temperature some spectral lines are difficult to separate into the components due to line broadening. At low temperatures, a large number of additional lines appear in the spectra of Tb and Gd compounds as a result of the structural phase transition, which complicates the interpretation of the spectrum.

In $SmFe_3(BO_3)_4$ as well as $GdFe_3(BO_3)_4$ (Ref. 11) crystals, only the LO component has been observed for the E mode at 489.2 cm^{-1} (Table 1). When using the measurement geometry with $\theta = 45°$, the energy of this mode is significantly shifted to lower frequencies (Figs. 1(a) and 2(a)). From the magnitude of the offset, an approximate position of the TO component, which is either hidden by the wing of an intense line at 442.0 cm^{-1} or has a low intensity, can be estimated. The absence of this line in IR spectra does not allow comparison with the data obtained from Raman spectra.

In addition to the above $7A_1 + 19E$ vibrational modes, in Raman spectra in the region of internal vibrations of BO_3 groups, we found three additional lines (Fig. 1(b), see Table 2). For Sm^{3+} ions in the range 1090–1290 cm^{-1}, additional spectral lines due to the excitation of electronic transitions can be expected.[8] However, the additional lines are observed at room temperature (Fig. 2(b), Table 2), which is not common for electron scattering. In Ref. 12 we have studied the temperature dependence of scattering spectra in $TbFe_3(BO_3)_4$ in the region of external vibrations. In the present paper, spectra of this compound in the region of internal vibrational

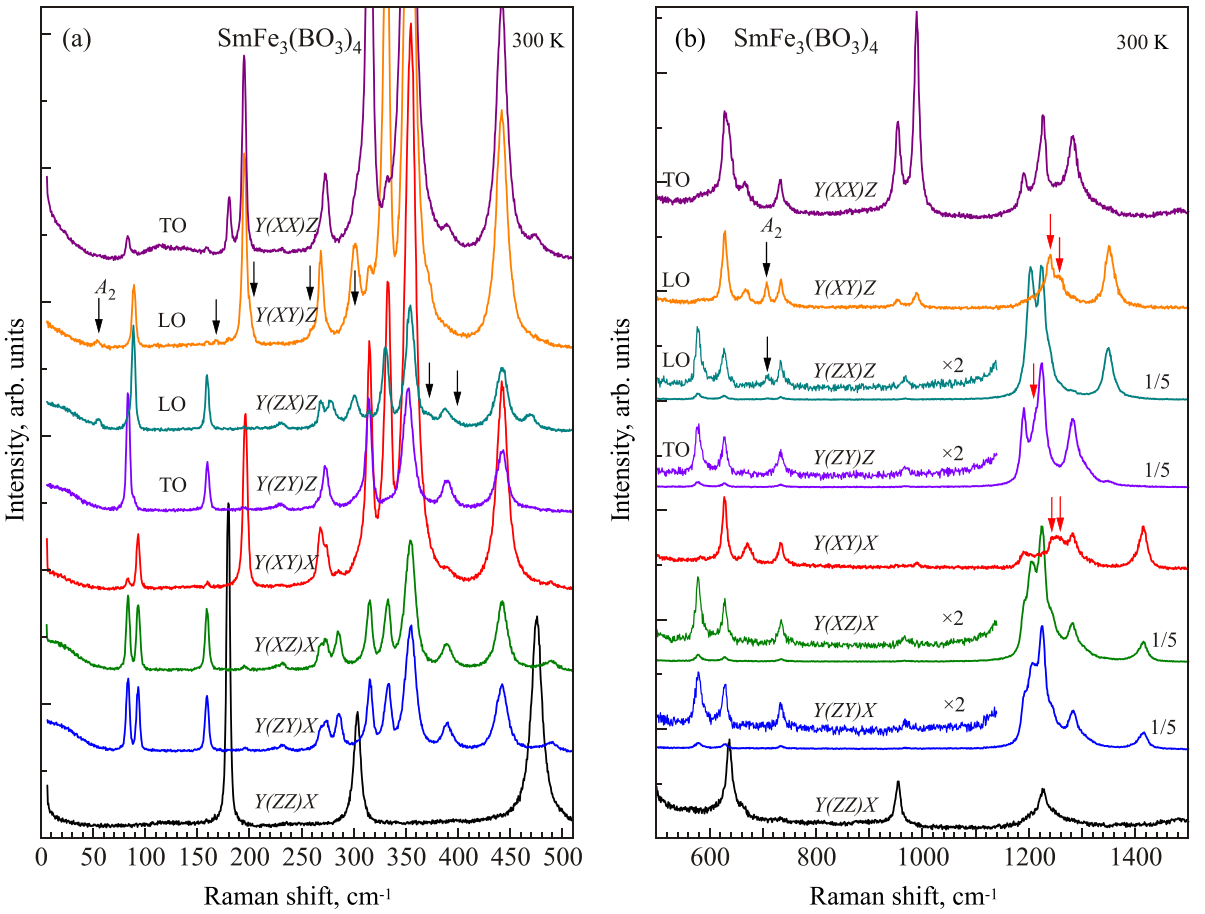

FIG. 2. Raman spectra of different polarizations observed in single-crystal $SmFe_3(BO_3)_4$ at 300 K in various geometries in the regions of external (a) and internal (b) BO_3 vibrational modes; $\lambda_{exc} = 532$ nm (38 mW); spectral resolution of 3.0 cm^{-1}.

modes were obtained (Fig. 3) and registered under the same conditions and geometries, as for $SmFe_3(BO_3)_4$. As shown in Fig. 3 and Table 2, in $TbFe_3(BO_3)_4$ three additional lines were also observed in this region. Thus, we can assume that these lines are not unique to this particular sample, but rather common for the entire class of these compounds.

Furthemore, in Ref. 11 in the region of the ν_3-BO_3 oscillation band for a number of crystals of this family, an additional mode has been observed in the spectra with $ZX + ZY$ polarizations. The authors have suggested that the appearance of this line may be due to Fermi resonance between the ν_3-vibration and a harmonic of the ν_4-vibration. To our knowledge, this most intense line of the three additional lines in the $\theta = 45°$ spectra of both crystals is shifted by about 4 cm^{-1} to lower frequencies and, according to the polarization rules, behaves as an LO component (Figs. 1(b), 2(b),

TABLE 1. Energies (cm^{-1}) of the observed A_1 and E external vibrational modes in single-crystal $SmFe_3(BO_3)_4$ at 300 K, compared to the literature data. The energies of the above modes at low temperatures are shown in brackets.

$SmFe_3(BO_3)_4$ (present paper) 300 K (10 K)		$TbFe_3(BO_3)_4$ [Ref. 12], 300 K (2 K)		$GdFe_3(BO_3)_4$ [Ref. 11], 300 K		$SmFe_3(BO_3)_4$ [Ref. 13], 300 K
A_1		A_1		A_1		
179.7 (179.5)		180.6 (182.4)		180		
302.3 (303.4)		308.2 (310.4)		307		
475.3 (478.4)		476.0 (474.5)		475		
E_{TO}	E_{LO}	E_{TO}	E_{LO}	E_{TO}	E_{LO}	E_{TO}
83.5 (81.8)	93.2 (92.3)	84.2 (89.1)	93.6(97.0)	84	93	85.1
	159.4 (160.7)		159.9 (158.5)	160	160	…
194.8 (193.4)	195.8 (194.4)	197.1 (199.0)	198.3 (199.8)	195	198	194.7
	231.0 (137.0)		230.4 (235.0)		232	229.7
264.3 (264.1)	268.4 (268.5)		269.4 (274.0)	270	270	265.2
273.5 (274.4)	285.5 (285.5)	273.5 (278.1)	289.0 (291.3)	273	287	279.2
315.1 (315.2)	332.7 (334.0)	315.4 (318.4)	330.4 (332.1)	315	330	313.7
352.4 (355.4)	355.4 (358.5)	350.7 (349.3)	355.8 (351.5)	352	357	382.3
	389.5 (394.4)		394.2 (403.5)	391	391	409.0
	442.0 (445.4)		445.0 (450.3)	443	443	438.5
	489.2 (491.2)		489.0 (492.0)		488	…

TABLE 2. Energies (cm^{-1}) of the observed A_1 and E internal vibrational modes in a single-crystal $SmFe_3(BO_3)_4$ at 300 K, compared to the literature data. The energies of the above modes at 10 K are shown in brackets.

$SmFe_3(BO_3)_4$ (present paper) 300 K (10 K)		$TbFe_3(BO_3)_4$ (present paper) 300 K		$GdFe_3(BO_3)_4$ [Ref. 11], 300 K		$SmFe_3(BO_3)_4$ [Ref. 13], 300 K
A_1		A_1		A_1		
636.9 (636.5)		637.5		638		
954.0 (952.6)		959.0		957		
989.0 (989.4)		989.3		990		
1227.0 (1231.0)		1234.5		1230		
E_{TO}	E_{LO}	E_{TO}	E_{LO}	E_{TO}	E_{LO}	E_{TO}
	578.5 (579.0)		580.0		580	576.5
	628.5 (629.8)		631.6	631	633	
666.5 (669.5)	671.2 (673.8)	670.5	674.5	670	676	669.5
	733.8 (734.8)		733.5		735	732.8
	967.5 (968.0)		966.5		968	979.5
1190.5 (1190)	1204.5 (1202)	1201.5	1216.5	1198	1212	1197.3
	1224.5 (1226.0)		1233		1229	1232.8
1282 (1283.5)	1415 (1416.5)	1278.0	1414.5	1280	1414	1295.6
additional lines		additional lines		additional lines		
	1211.5 (1214)		~1221			
	1243.5 (1245)		1246		1250	
	1259 (1261)		1260			

and 3). For the vibrational mode with an energy of about 630 cm^{-1}, a harmonic of which falls within this range, splitting into TO and LO components is either negligible or not observable experimentally (Table 2). Moreover, the mechanism proposed in Ref. 11 can only explain a single additional line, but not three. It should also be noted that for the highest frequency E mode, the TO component line has an asymmetry in the high frequency region, while the LO component line exhibits an asymmetry in the low frequency region. This is likely due to the presence of two extra lines corresponding to the TO and LO components of the E mode, additionally to those specified in Table 2. As a result of the spectral analysis, we found that besides the main spectrum in this region, consisting of three E modes, there are three additional E modes, which are shifted in energy and exhibit slightly different splittings into the TO and LO components. Thus, the spectrum contains additional vibrations of BO_3 groups in this energy region, but in a different crystalline environment.

Additional phonon lines in the region of the ν_3 oscillation of BO_3 groups in the crystals under study may be also associated with the presence of impurities. The possibility of molybdenum and bismuth impurities has been discussed in a number of studies.[16–18] In particular, in Ref. 16 three nonequivalent Tb^{3+} ions have been observed in the EPR spectra of $TbFe_3(BO_3)_4$ crystal, two of which have been attributed by the authors to the presence of bismuth and molybdenum in the neighboring positions. In Ref. 17 in the absorption spectra in the region of the $^7F_3$ transition of Tb^{3+} ions, several additional lines shifted from the main ones by 5.8–11.5 cm^{-1} have been observed and attributed by the authors to the presence of bismuth and molybdenum impurities. In the same paper, the results of Ref. 18, where additional lines shifted by 10 cm^{-1} with respect to the main ones were observed in the region of the $^5D_4$ term of Tb^{3+} in absorption spectra, have also been interpreted in terms of the presence of impurities.

The reason for the observation of three additional lines in this specific spectral region can be understood from the following considerations. Firstly, upon isomorphic substitution of Sm with Tb (Tables 1 and 2), not only external but also internal vibrational modes of BO_3 groups shift their positions, which is especially noticeable in the region of ν_3 oscillation. In particular, for the LO and TO components at 1190.5 cm^{-1} and 1204.5 cm^{-1}, a shift of 11 cm^{-1} and 12 cm^{-1}, i.e., about

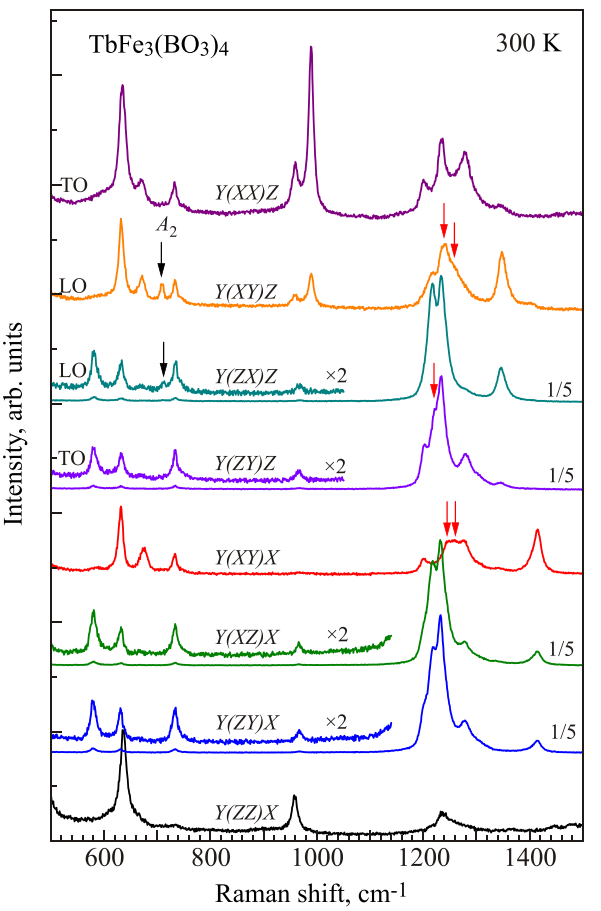

FIG. 3. Raman spectra of different polarizations observed in single-crystal $TbFe_3(BO_3)_4$ at 300 K in various geometries in the region of internal vibrational modes of BO_3; $\lambda_{exc} = 532$ nm (38 mW); spectral resolution of 3.0 cm^{-1}.

TABLE 3. Energies (cm^{-1}) of the observed A_2 vibrational modes ($\theta = 45°$) in single-crystal $SmFe_3(BO_3)_4$ at 300 K, compared to the literature data. The energies of the above modes at 10 K are shown in brackets.

$SmFe_3(BO_3)_4$ (present paper) 300 K (10 K)	$TbFe_3(BO_3)_4$ [Ref. 12], 300 K	$SmFe_3(BO_3)_4$ [Ref. 13], 300 K	$SmFe_3(BO_3)_4$ [Ref. 21], 5 K
A_2 ($\theta = 45°$)	A_2 ($\theta = 45°$)	A_2	A_2
54.8 (52.0 at 45 K)	60.5	52.1	48.6 (TO) 61.5 (LO)
168 (169.9)	…	164.6	~171.5
201.1 (201.3)	205.4	197.8	~205
259.2 (-)	258.5	256.0	
300.9 (303.2)	301.4	292.1	
371.8 (377.8)	372.6	370.3	
397.4 (401.5)	…	398.0	
….	….	….	
		670.9	
708.0 (709.4)	709.5	735.3	
		765.1	
		1222.8	

1%, was observed (Table 2). For the external vibrational modes, a relative shift of more than 1% was only observed for one A_1 mode (303.2 cm^{-1}) and two E modes (194.8 and 389.5 cm^{-1}). This behavior of the lines upon the isomorphic substitution may indicate that BO_3 groups cannot be considered as "rigid" entities, in which the energies of internal vibrational modes remain virtually unchanged. Secondly, the ν_3 oscillation, which is the most sensitive among the internal vibrations to a change in the crystal field, has the highest energy. Upon the same (in percentage terms) shift of the additional vibrational modes with respect to the main ones, the absolute shift becomes sufficient for their observation. Moreover, the additional lines are not covered by the main ones. Thirdly, the substitution of Sm or Fe with an impurity ion causes distortion of six BO_3 groups at once. In this case, the intensity ratio of the main and additional lines is higher for BO_3 oscillations (both internal and external), as compared with Fe vibrations. Thus, we believe that the observed additional modes are associated with the vibrations of BO_3 groups near an impurity center.

In addition to the discussed above $7A_1 + 19E$ main and $3E$ additional vibrational modes, the $\theta = 45°$ spectra corresponding to the LO components exhibit a series of weak lines, which are denoted in Figs. 1–3 with black arrows. They are assigned to polar A_2 modes, "forbidden" by the selection rules for inelastic scattering at $\theta = 0°$ and $\theta = 90°$. The possibility of observing the inactive A_2 polar oscillations in the $\theta = 45°$ geometry due to their interaction with active E modes has been shown for alpha quartz.[19,20] The energies of the A_2 vibrational modes observed at $\theta = 45°$ for crystalline $SmFe_3(BO_3)_4$ are shown in Table 3. For comparison, it also shows the data for $TbFe_3(BO_3)_4$ obtained from similar Raman measurements,[12] as well as the data on IR absorption[13] and absorption in the submillimeter range[21] for the crystal under study. As can be seen from Table 3, for the Sm compound in the region of external vibrations (up to 500 cm^{-1}), as in IR measurements, one of the A_2 vibrational modes is not observed. Previously, for the Tb compound, we have obtained for A_2 modes the values of 277.2 and 470 cm^{-1}, besides those shown in Table 3. However, comparing the spectra and the energies of vibrational modes in Sm and Tb compounds, it can be assumed that those are the LO components of E modes at $\theta = 45°$. The ambiguity in attributing weak additional lines in the spectra of $TbFe_3(BO_3)_4$ crystal is related to the fact that the LO components of E modes (289 and 489 cm^{-1}) with the ZX- and ZY-polarizations disappear at $\theta = 45°$, while lines in XY- and YY-spectra emerge.[12] For crystalline $SmFe_3(BO_3)_4$, such interplay between the intensities in the spectra with different scattering tensor components was not observed.

Previously, in crystalline $TbFe_3(BO_3)_4$, a shift of two phonon lines at temperatures below T_N has been observed.[12] We also expected to find such a manifestation of a magnetic transition for the compound under study. However, upon the

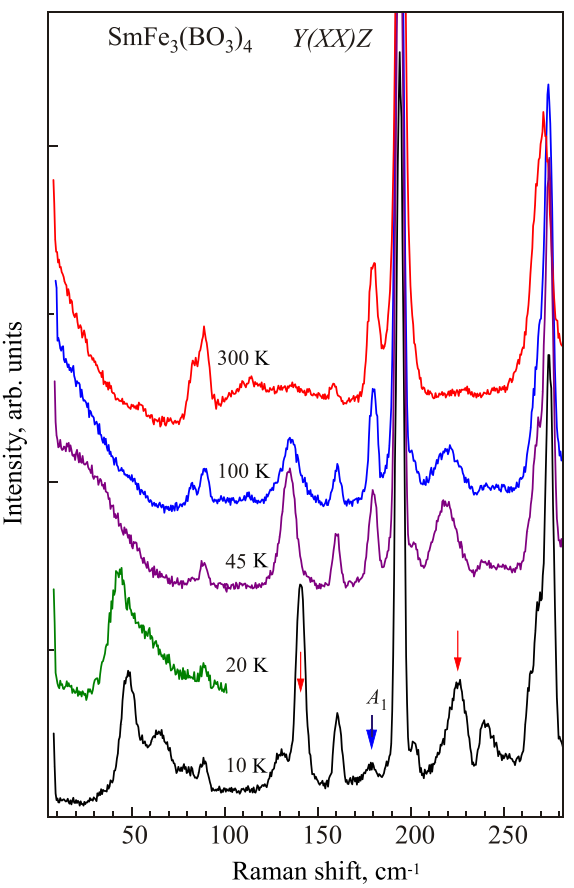

FIG. 4. Temperature behavior of the Raman spectra of single-crystal $SmFe_3(BO_3)_4$ in the $Y(XX)Z$ geometry; $\lambda_{exc} = 532$ nm (38 mW); spectral resolution of 3.0 cm^{-1}.

transition to a magnetically ordered state in crystalline $SmFe_3(BO_3)_4$, phonon lines do not experience (within the measurement accuracy) any frequency shifts. As shown in Fig. 4, only the intensity of the A_1 mode (179.7 cm^{-1}) reacts to the magnetic transition. Above T_N its intensity shows normal behavior, while below T_N the intensity of this line in *XX*- and *YY*-spectra is significantly reduced. The *E* mode with a frequency of 159.4 cm^{-1} (Fig. 4) also exhibits an anomalous temperature dependence of the intensity over the entire temperature range, but does not respond within the measurement accuracy to the magnetic transition.

Two-magnon light scattering

Below the transition temperature to the magnetically ordered state, in the low-frequency region of Raman spectra of $SmFe_3(BO_3)_4$, a broad band of complex shape, corresponding to two-magnon light scattering (Fig. 1(a)) was observed. As seen in Fig. 4, with increasing temperature the band shape changes, and above T_N, up to room temperature, the band is observed as a wing of the Rayleigh line. As shown in Fig. 5(a), the Raman spectra have a complex shape and are observed with all the components of the scattering tensor (except *ZZ*) and, of course, can be attributed to two-magnon scattering. Furthermore, each of the above spectra can be decomposed into four bands with energies 48.0, 55.5, 65.0, and 79.5 cm^{-1} (denoted in Fig. 5(a) with arrows), which are present in all the spectra, but with varying intensity. Above T_N the two-magnon scattering spectra with these above components of the scattering tensor are transformed into a broad band centered at zero energy (Fig. 5(b)).

Unlike Nd, Gd, Tb, Er, and Y ferroborates,[11,12] in which the two-magnon scattering has been observed only in the spectra with *XZ*- and *YZ*-polarizations, two-magnon scattering in the spectra of samarium ferroborate is observed for both off-diagonal and diagonal components of the scattering tensor (all components, except *ZZ*). This difference may be due to the specific aspects of the magnetic structure of Sm ferroborate, in which the Fe and Sm sublattices are not collinear, but turned by 70° relative to each other.[7] The complex shape of the two-magnon spectrum reflects the features in the density of states of the magnon branches. Evaluation of the magnon energy on the boundary of the Brillouin zone gives $E_m \sim 47$ cm^{-1}.

Structure of the ground multiplet $^6H_{5/2}$ of a Sm^{3+} ion

The crystal field of D_3 symmetry in $SmFe_3(BO_3)_4$ splits the ground state multiplet $^6H_{5/2}$ of a Sm^{3+} ion with an odd number of electrons into Γ_4 and Γ_{56} Kramers doublet. The energies of the Stark levels of the ground multiplet $^6H_{5/2}$, determined from the temperature dependence of the absorption spectra of polarized radiation, are as follows: 0 (Γ_4), 135 (Γ_{56}), and 220 (Γ_4) cm^{-1} in the paramagnetic state.[8,9] Upon the transition to the magnetically ordered state, the exchange splitting of the Stark levels occurs with the magnitude of 13.2 cm^{-1} for the ground level (for the other two, it is not essential).[8,9] The magnitudes of the exchange splitting of Kramers doublets Δ_{exp} (cm^{-1}), both determined from the

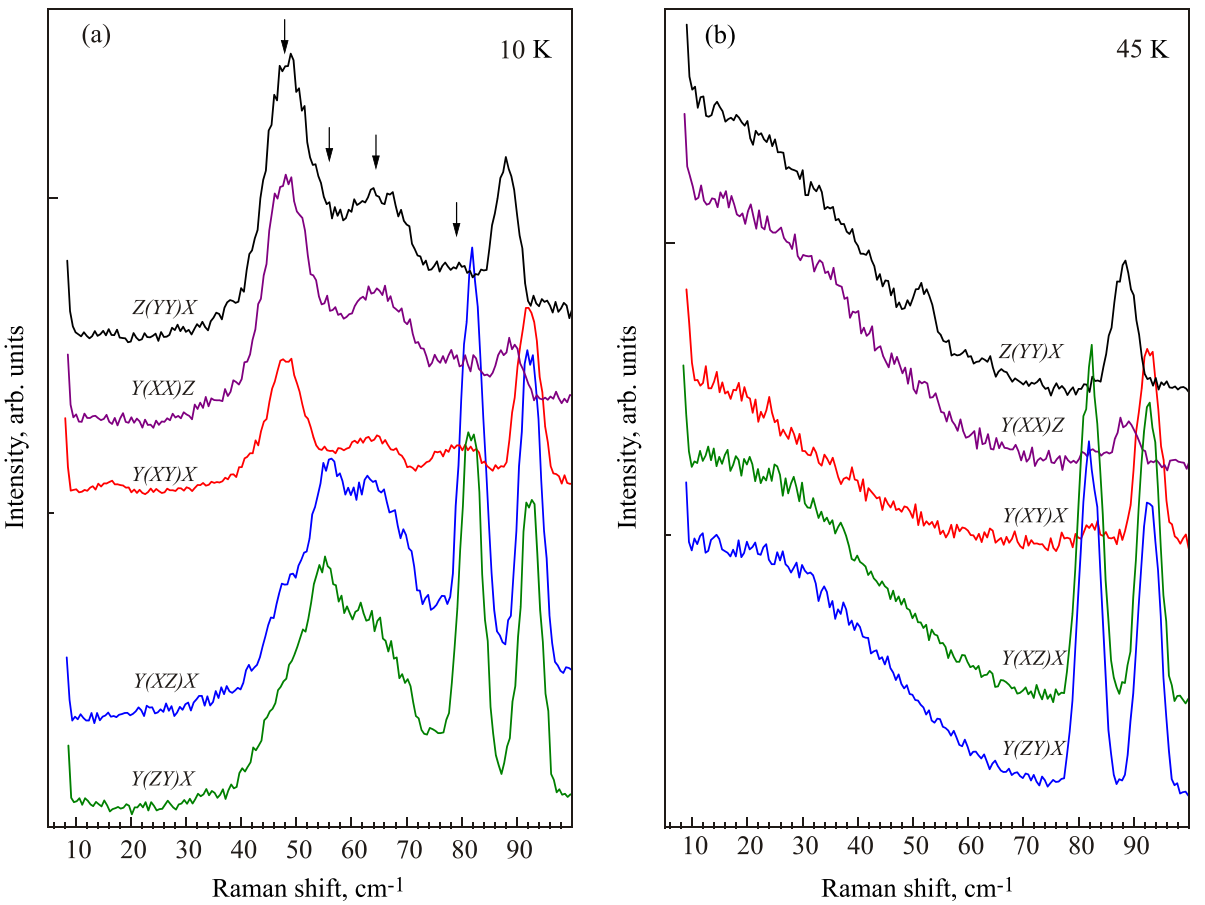

FIG. 5. Raman spectra of different polarizations observed in single-crystal $SmFe_3(BO_3)_4$ in the region of two-magnon scattering in various geometries and at different temperatures: 10 K (a), 45 K (b); $\lambda_{exc} = 532$ nm (38 mW); spectral resolution of 5.0 cm^{-1}.

low-temperature spectra ($T = 5$ K) and calculated Δ_{th} (cm^{-1}), as well as the measured shifts of the doublet gravity centers δE_{exp} (cm^{-1}) at $T = 5$ K and the respective calculated δE_{th} (cm^{-1}) induced by the exchange interaction, have been presented in Ref. 8.

Figure 6(a) shows the Raman spectra of a $SmFe_3(BO_3)_4$ single crystal in the region of the transitions within the ground multiplet of Sm^{3+} ions with different polarizations obtained with spectral resolution of 3 and 2 cm^{-1} at a temperature of 10 K. The inset shows the scheme of the experimentally observed transitions. As shown in Fig. 6(a), in the low-frequency region of the spectrum, there are two lines corresponding to the transitions with energies of 9.9 cm^{-1} ($Y(ZY)X$ scattering geometry) and 16.0 cm^{-1} ($Y(XY)X$ scattering geometry). At low temperatures, the spectra with XY-, XX-, and YY-components of the scattering tensor show a strong line corresponding to the transition of energy 140.8 cm^{-1} from the ground state to the first excited level. In addition, on the low-frequency side of this line (Fig. 6(a)), there are two more weak lines (125.5 and 130.9 cm^{-1}) corresponding to the thermally activated transitions from the excited states at 9.9 and 16.0 cm^{-1} to the level of 140.8 cm^{-1} (see the transition schematics in the inset in Fig. 6(a)).

The temperature evolution of the scattering spectra in the region of electron transitions is shown in Fig. 6(b). As the temperature rises the intensity of thermally activated transitions increases and, in terms of energy, they approach the transition from the ground state. Above T_N only a single line (135.1 cm^{-1}) is observed, which corresponds to the transition from the ground state to the first excited state in the paramagnetic phase. For the next excited state in the region of 220 cm^{-1}, one thermally activated transition can also be distinguished at low temperatures (Fig. 6(b)); its temperature evolution is the same as described above. Furthermore, as seen in the figure, there is a strong electron-phonon coupling between the electronic transition at 225.6 cm^{-1} and the phonon mode at 237.0 cm^{-1}. When the temperature is lowered and the electronic transition is shifted to higher energy due to splitting of the ground state by the exchange field, a strengthening of the electron-phonon interaction occurs below T_N and, as a consequence, the intensity of the phonon line increases. In this case, the shape of the phonon line is described by the Fano function.

In the study of the absorption spectra in the submillimeter region in $SmFe_3(BO_3)_4$ in the magnetically ordered state, several absorption bands have been observed in Ref. 10. For $h \parallel c$ the observed ω_+^{Sm} mode at 16.6 cm^{-1} has been attributed by the authors of Ref. 10 to the electronic transitions within the Kramers doublet of Sm^{3+}. The fact that its frequency exceeds the magnitude of the exchange splitting of the 13.2 cm^{-1} doublet is, according to the authors,[10] due to the interaction with the low-lying antiferromagnetic resonance mode. For $h \parallel c$ two modes have been observed: $\omega_+ = 12.7$ cm^{-1} (only at 4.2 K) and $\omega_- = 10.8$ cm^{-1}. The appearance of these modes is due to coupled oscillations of Fe^{3+} and Sm^{3+} spins. The classification of the modes as "rare-earth" and "antiferromagnetic

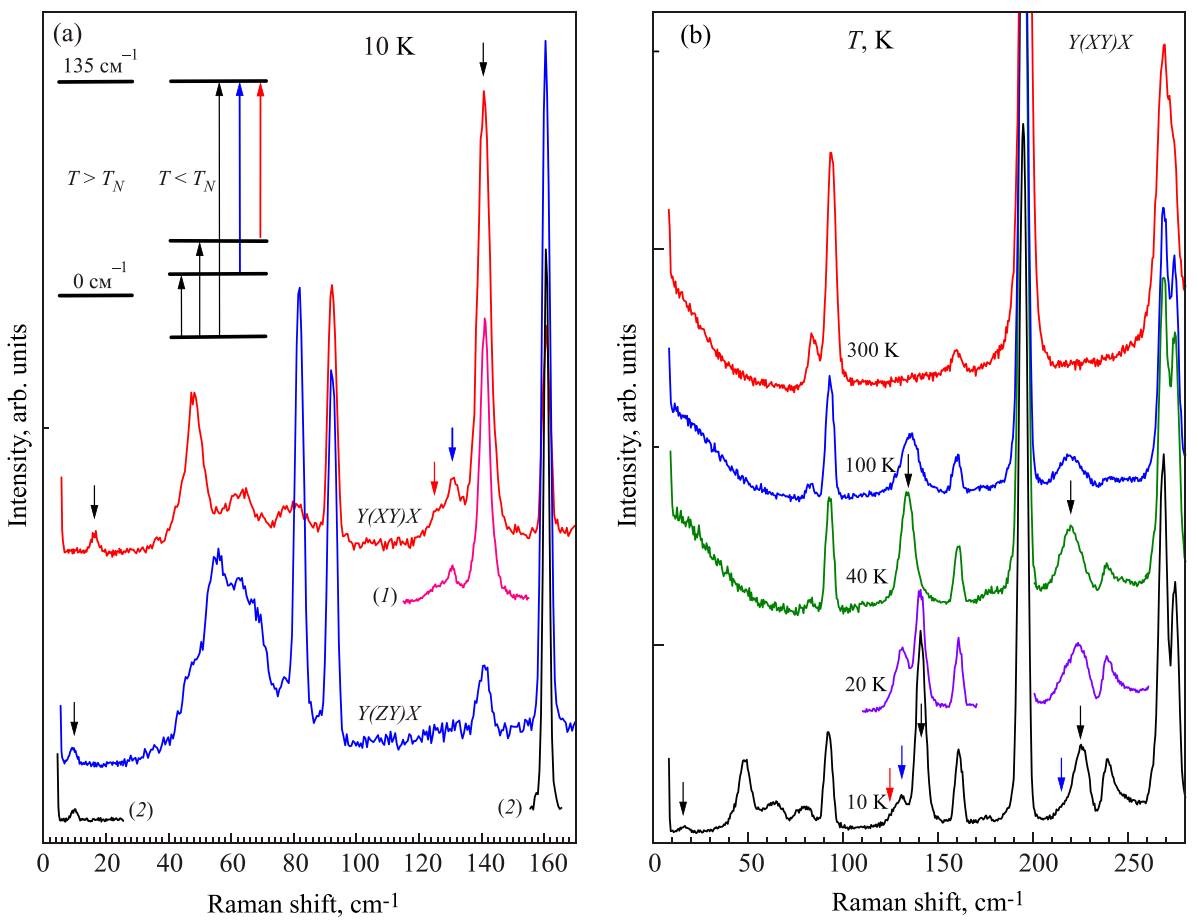

FIG. 6. Raman spectra of different polarizations observed in single-crystal $SmFe_3(BO_3)_4$: (a) at 10 K, $Y(XY)X$ and $Y(ZY)X$, spectral resolution of 3.0 cm^{-1} (2 cm^{-1} resolution for spectra (*1*) and (*2*)), the inset shows schematics of the observed transitions; (b) temperature dependence of the spectra in the region of two-magnon scattering and the levels of the ground multiplet of $SmFe_3(BO_3)_4$ in the $Y(XY)X$ scattering geometry; spectral resolution of 5.0 cm^{-1}.

TABLE 4. Energies (cm^{-1}) of the observed electronic transitions of a Sm^{3+} in single-crystal $SmFe_3(BO_3)_4$ at low temperatures, compared to the literature data.

Present paper		Ref. 9		Ref. 10
10 K	40 K	5 K	40 K	4.2 K
9.9	0		0	10.8
		13.2		~12.7
16.0				16.6
125.5	135.1		135	
130.9				
140.8				
215.7	220.0		220	
225.6				

resonance" is rather artificial, since coupled oscillations of Fe and Sm ions are realized in this case.[10]

Table 4 shows the observed energies of the electronic transitions of a Sm^{3+} ion in a $SmFe_3(BO_3)_4$ crystal at low temperatures in comparison with the literature data. As can be seen from the table, our data in the region of the ground state do not match the results of Ref. 9. Our magnitudes of the energies of low-frequency transitions correspond with an accuracy of 0.1 cm^{-1} to the energy values of Ref. 10 at 9 K. The observation of two excitations with energies of 9.9 and 16.0 cm^{-1} in the low-energy region confirms the presence of a strong magnetic interaction between the subsystems of Sm and Fe ions.

Conclusion

For the first time, the Raman studies of samarium ferroborate were conducted. All the modes predicted by the group-theory analysis for a given symmetry of the crystal, $7A_1 + 19E$, were observed. The splitting between the LO and TO components of polar E phonons was determined. Using different scattering geometries, the energies of 8 out of 12 A_2 modes, forbidden in Raman scattering, were obtained.

In the region of stretching vibration of BO_3, several additional E modes were found, which appear, in our opinion, due to the presence of impurity centers in these crystals. Analysis of the results presented in this work and published data indicate that the presence of impurities is, probably, characteristic for a number of compounds of this family and not a property of the specific sample.

Under the transition to a magnetically ordered state, an anomalous behavior of the intensity of the line corresponding to the vibrational mode A_1 was found. The energy of the E and A_1 phonon modes did not respond to the magnetic transition within the measurement accuracy, unlike in the case of a $TbFe_3(BO_3)_4$ crystal.[12] The intensity variation of this line reflects the change in the crystal field, which might be associated with the magnetoelectric effect upon the transition to the magnetically ordered state.

It was shown that at a low temperature, the spectrum of two-magnon excitations has a complex shape and is observed, unlike in Nd, Gd, Tb, Er, and Y ferroborates, with both off-diagonal and diagonal components of the scattering tensor. This difference is possibly due to the peculiarities of the magnetic structure of Sm ferroborate, in which Fe and Sm sublattices of are not collinear but rotated by 70° with respect to each other.[7] The complex shape of the two-magnon spectrum reflects the features in the density of states of the magnon branches. The magnon energy E_m at the Brillouin zone boundary was estimated as ~47 cm^{-1}.

The structure of the ground multiplet $^6H_{5/2}$ of a Sm^{3+} ion in the paramagnetic and antiferromagnetic states and the effect of the magnetic phase transition were studied. The fact that two excitations with energies of 9.9 and 16.0 cm^{-1} were observed in the low-energy region of the spectrum confirms the presence of a strong magnetic interaction between Fe and Sm subsystems.

[a]Email: peschansky@ilt.kharkov.ua

[1]A. M. Kadomtseva, Yu. F. Popov, S. S. Krotov, G. P. Vorob'ev, E. A. Popova, A. K. Zvezdin, and L. N. Bezmaternykh, Fiz. Nizk. Temp. **31**, 1059 (2005) [Low Temp. Phys. **31**, 807 (2005)].
[2]A. M. Kadomtseva, Yu. F. Popov, G. P. Vorob'ev, A. P. Pyatakov, S. S. Krotov, K. I. Kamilov, V.Yu. Ivanov, A. A. Mukhin, A. K. Zvezdin, A. M. Kuz'menko, L. N. Bezmaternykh, I. A. Gudim, and V. L. Temerov, Fiz. Nizk. Temp **36**, 640 (2010) [Low Temp. Phys. **36**, 511 (2010)].
[3]A. K. Zvezdin, G. P. Vorob'ev, A. M. Kadomtseva, Yu. F. Popov, A. P. Pyatakov, L. N. Bezmaternykh, A. V. Kuvardin, and E. A. Popova, Pis'ma Zh. Eksp. Teor. Fiz. **83**, 600 (2006) [JETP Lett. **83**, 509 (2006)]].
[4]A. I. Popov, D. I. Pimenov, and A. R. Zvezdin, Phys. Rev. B **87**, 024413 (2013).
[5]A. A. Mukhin, G. P. Vorob'ev, V. Yu. Ivanov, A. M. Kadomtseva, A. S. Narizhnaya, A. M. Kuz'menko, Yu. F. Popov, L. N. Bezmaternykh, and I. A. Gudim, Pis'ma Zh. Eksp. Teor. Fiz. **93**, 305 (2011) [JETP Lett. **93**, 275 (2011)].
[6]Yu. F. Popov, A. P. Pyatakov, A. M. Kadomtseva, G. P. Vorob'ev, A. K. Zvezdin, A. A. Mukhin, V.Yu. Ivanov, and I. A. Gudim, Zh. Eksp. Teor. Fiz. **138**, 226 (2010) [J. Exp. Theor. Phys. **111**, 199 (2010)].
[7]C. Ritter, A. Pankratas, I. Gudim, and A. Vorotilov, J. Phys.: Condens. Matter. **24**, 386002 (2012).
[8]M. N. Popova, E. P. Chukalina, B. Z. Malkin, D. A. Erofeev, L. N. Bezmaternykh, and I. A. Gudim, Zh. Eksp. Teor. Fiz. **145**, 128 (2014) [J. Exp. Theor. Phys. **118**, 111 (2014)].
[9]E. P. Chukalina, M. N. Popova, L. N. Bezmaternykh, and L. A. Gudim, Phys. Lett. A **374**, 1790 (2010).
[10]A. M. Kuz'menko, A. A. Mukhin, V. Yu. Ivanov, A. M. Kadomtseva, S. P. Lebedev, and L. N. Bezmaternykh, Pis'ma Zh. Eksp. Teor. Fiz. **94**, 318 (2011) [JETP Lett. **94**, 294 (2011)].
[11]D. Fausti, A. A. Nugroho, P. H. M. van Loosdreht, S. A. Klimin, and M. N. Popova, Phys. Rev. B **74**, 024403 (2006).
[12]A. V. Peschanskii, A. V. Yeremenko, V. I. Fomin, L. N. Bezmaternykh, and I. A. Gudim, Fiz. Nizk. Temp. **40**, 219 (2014) [Low Temp. Phys. **40**, 171 (2014)].
[13]K. N. Boldyrev and D. A. Erofeev, Opt. Spektrosk. **116**, 948 (2014) [Opt. Spectrosc. **116**, 872 (2014)].
[14]I. A. Gudim, E. V. Eremin, and V. L. Temerov, J. Cryst. Growth **312**, 2427 (2010).
[15]H. Poulet and J.-P. Mathieu, *Spectres de Vibration et Symetrie des Cristaux* (Cordon and Breach, Paris, 1970).
[16]V. A. Bedarev, M. I. Paschenko, M. I. Kobets, K. G. Dergachev, V. A. Paschenko, A. N. Bludov, E. N. Khatsko, S. L. Gnatchenko, L. N. Bezmaternykh, and V. L. Temerov, Fiz. Nizk. Temp. **39**, 219 (2013) [Low Temp. Phys. **39**, 167 (2013)].
[17]M. N. Popova, T. N. Stanislavchuk, B. Z. Malkin, and L. N. Bezmaternykh, J. Phys.: Condens. Matter **24**, 196002 (2012).
[18]A. V. Malakhovskii, S. L. Gnatchenko, I. S. Kachur, V. G. Piryatinskaya, A. L. Sukhachev, and V. L. Temerov, Eur. Phys. J. B **80**, 1 (2011).
[19]S. M. Shapiro and J. D. Axe, Phys. Rev. B **6**, 2420 (1972).
[20]W. Hayes and R. Loudon, *Scattering of Light by Crystals* (John Wiley and Sons, New York, 1978).
[21]K. N. Boldyrev, T. N. Stanislavchuk, A. A. Sirenko, L. N. Bezmaternykh, and M. N. Popova, Phys. Rev. B **90**, 121101 (2014).

Translated by L. Gardt